Progress In Electromagnetics Research M, Vol. 22, 259–269, 2012

HUMAN BODY IMPACT ON UWB ANTENNA RADIATION

A. Vorobyov[1, 2, *] and A. Yarovoy[2]

[1]Institut d'Electronique et de Télécommunications de Rennes, UMR CNRS 6164, Université de Rennes 1, Rennes Cedex 35042, France

[2]Delft University of Technology, International Research Center for Telecom and Radar (IRCTR), Mekelweg 4, CD Delft 2628, the Netherlands

Abstract—We experimentally quantify the radiation of a small Ultra-Wideband (UWB) antenna placed on a human body. The measurements are performed for different antenna locations on the body, namely the head, torso and belt. First the antenna is measured in free space as reference, and then the influences of the body are investigated for different frequencies and antenna polarizations. We observe minimal signal blockage when the antenna is located on the head. It is around 5 dB–10 dB loss for all polarizations. For the belt and torso, the blockage is 10 dB to 35 dB, for both polarizations.

1. INTRODUCTION

UWB communication systems are characterized by a wide signal spectrum and low radiated power spectral density. Impulse radio [1] is one of the most interesting aspects of UWB radio systems, which might be used in multiple applications. One of the possible applications is body network [2]. The antenna plays a primary role in communication systems. Their design becomes more challenging for wearable devices where the influence of the body on the antenna characteristics, such as input impedance, current distribution, gain and radiation patterns, needs to be taken into account. UWB communication systems for personal wireless area network cannot be successfully implemented without achieving an understanding of the influence of the body on the antenna characteristics. Previous studies such as those described in [4–6] did not take into account the frequency dependency of the

Received 23 November 2011, Accepted 16 December 2011, Scheduled 27 December 2011
* Corresponding author: Alexander V. Vorobyov (alexander.vorobyov@gmail.com).

antenna radiation patterns and focused mainly on the typical LOS and NLOS channels. Others as [7, 8] considered this frequency dependency, and [2] showed that the human body had an impact on UWB antenna performances and, consequently, system design. In papers [12, 13], the authors investigated radiation efficiency of an internal handset antenna operating at the FM band.

But it is still not clear what values are of the human body influence on the antenna performance. In this paper, we are going to research influence of the human body on the antenna and demonstrate numerically what are the values of the human body influence (like the human body blockage or body energy absorption).

Thereto we perform measurements with available equipment and antennas. Antenna and measurement setup description are presented in the paper.

The paper is organized as follows. Section 2 describes the UWB antenna and their feed line. Section 3 focuses on the measurement setup. The measurement results are discussed in Section 4, and conclusions are given in Section 5.

2. UWB ANTENNA

Based on our experience with elliptically shaped dipoles [9], we have developed a so-called butterfly antenna to be used in UWB communications [10]. This antenna is capable of radiating a 200 ps monocycle pulse. The optimized length of the butterfly antenna is about 2.2 cm, and the optimal flair ellipticity is 0.9 (Fig. 1(a)).

The antenna was made for a project about impulse radio. For that purposes, the antenna is operating well in a frequency band 1 GHz to 5 GHz. Antenna radiation pattern and antenna gain are given in Figs. 1(b), (c).

When the antenna dimensions become comparable to those of the ground plane and feeding line, the common and differential mode currents have similar magnitudes, drastically changing the antenna properties. In order to increase the common mode impedance of the antenna, we propose a feeding line design based on the shielded loop [3]. The proposed shielded loop antenna feeding line design not only reduces the common mode current but also acts as antenna balancing (antenna balun), removing the need for an extra balun.

3. IMPULSE RADIO SETUP

The measurement setup is illustrated in Fig. 2. The pulse generator is connected to the transmit antenna via a 2 meter RF cable and

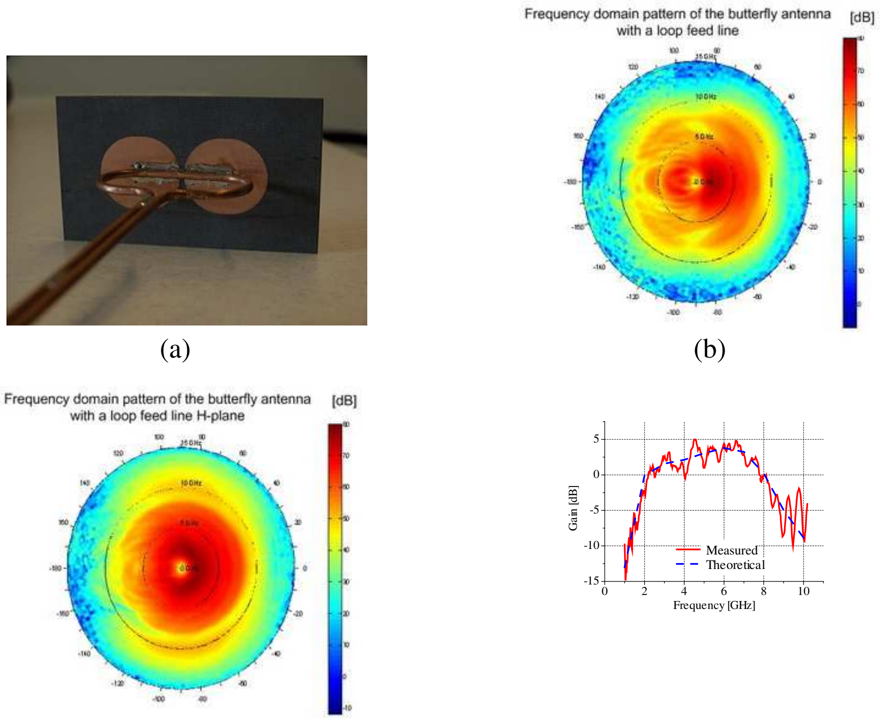

Figure 1. (a) Butterfly antenna with loop feeding, (b) measured radiation pattern: *E*-plane, (c) *H*-plane and (d) comparison theoretical/measured antenna gain.

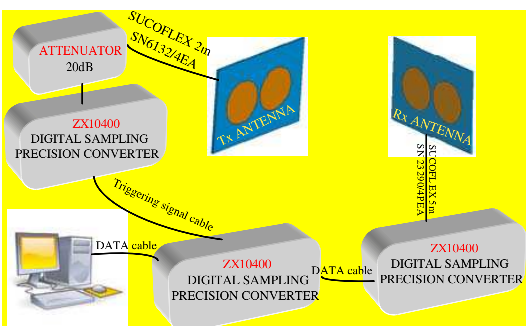

Figure 2. Time domain antenna measurement setup.

a 20 dB attenuator. The Antenna Under Test (AUT) is connected to the sampling unit by a 5 meter RF cable. The sampling unit is connected to the Digital Sampling Converter by custom data cables, and the digitized signal is then transferred to the PC running the data acquisition software (Marcha) using the LPT port.

The K263-2 generator can output three different waveforms, and the best suited to our antenna is the 220 ps Gaussian-like pulse shown in Fig. 3.

The E and H plane radiation patterns are measured in four scenarios. For reference, we measure the AUT mounted on a polystyrene column ($\varepsilon_r = 1$), which is rotated 360 degrees by 10 degree steps. For each angle, we measure the antenna response in time domain

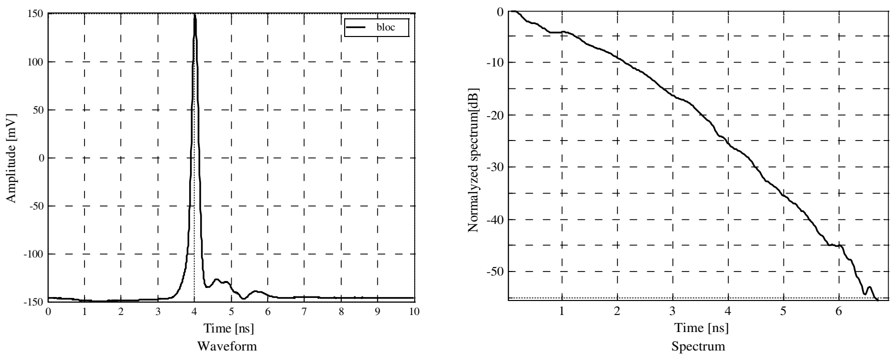

Figure 3. Pulse generator output waveform and spectrum.

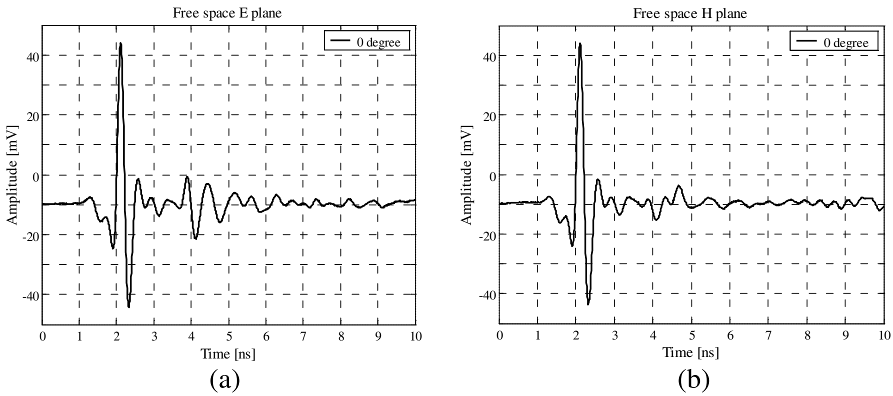

Figure 4. Measured waveforms. Antenna in a free space on a 3 m distance: (a) horizontal polarization and (b) vertical polarization.

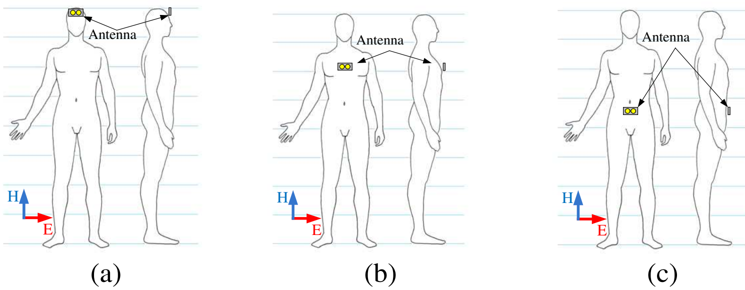

Figure 5. The three scenarios; head, torso and belt.

(1024 points in a 10 ns time window as shown in Figs. 3, 4). To avoid any influence on the antenna during the measurements, the polystyrene column has a 1.5 m height from the floor and is located about 2 m from any reflect surface. This distance was enough to separate the main pulse from any reflected pulse. The signal transmitted through the antenna pair by Tx-Rx antennas separation of 3 m is used as a reference signal. Its waveform and spectrum are shown in Fig. 4.

The measurement is then repeated with the antenna held by hand 5 cm away from the body in the belt and torso cases, and 7 cm away from the head as illustrated in Fig. 5.

4. MEASUREMENT RESULTS

Figure 6 shows the measured time signal waveforms at 0, 90, 180 and 270 degrees for three different scenarios. From the complete set of data we observe that the received waveforms have different shapes for different angles for the belt and torso scenarios in the E-plane, whereas they only differ in the back radiation direction (between 140 and 220 degree) in the H-plane. The magnitude of the received signal at 180 degree is comparable to the system's noise level. In the head scenario (Fig. 6(a)), the pulse shape remains similar for all angles in both E and H planes.

Figure 7 shows the peak-to-peak voltage amplitude measured at the receive antenna as a function of the azimuth angle for each scenario and in both planes.

It can be seen that in free space the butterfly antenna exhibits a typical dipole-like behavior, with an omnidirectional pattern in the H-plane and a figure of "8" pattern in the E-plane. The radiation in front of a body is slightly (1 dB–3 dB) increased and at the same time on back side decreased from -2 dB for head scenario and up to -40 dB

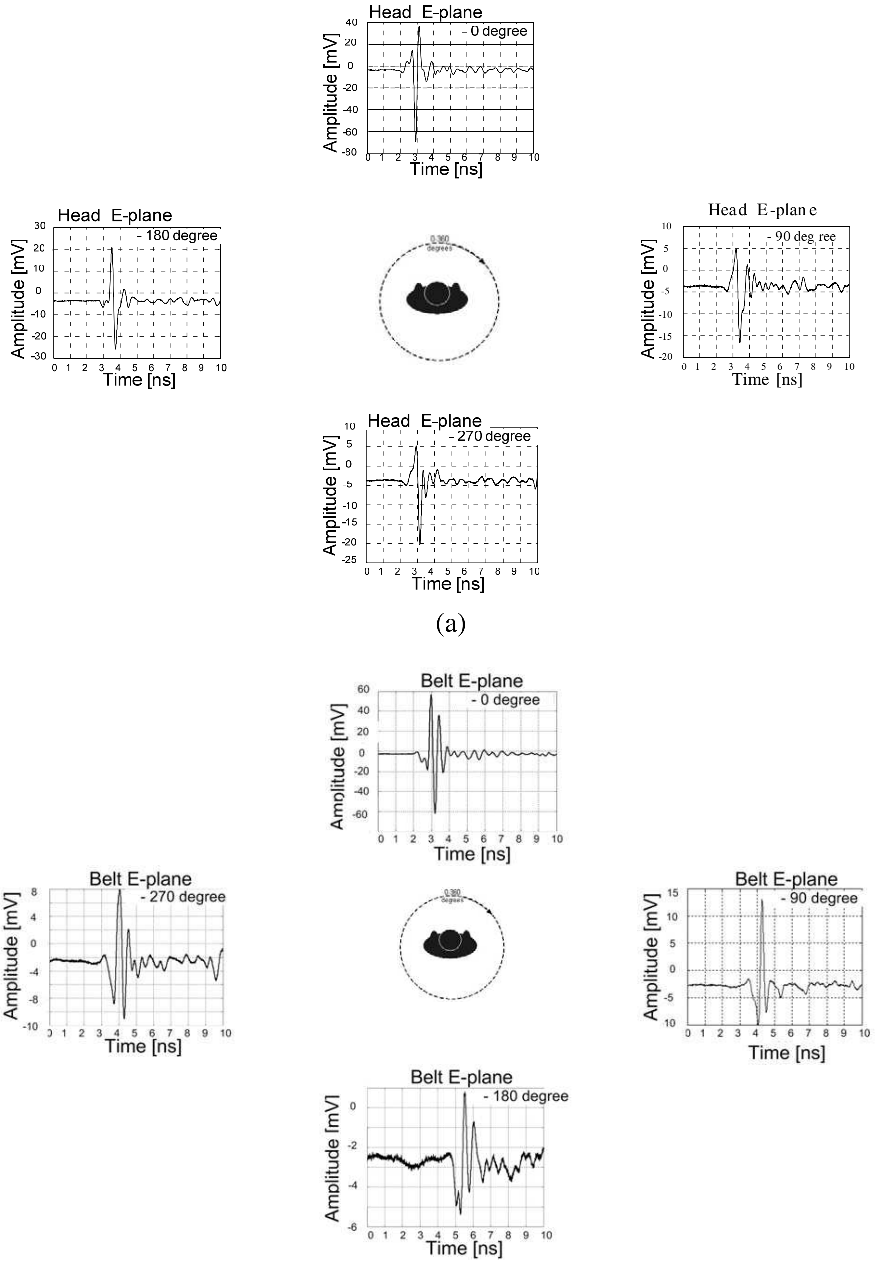
Head E-plane
- 0 degree
Amplitude [mV]
Time [ns]
Head E-plane
- 180 degree
Amplitude [mV]
Time [ns]
0..360 degrees
Head E-plane
- 90 degree
Amplitude [mV]
Time [ns]
Head E-plane
- 270 degree
Amplitude [mV]
Time [ns]
(a)
Belt E-plane
- 0 degree
Amplitude [mV]
Time [ns]
Belt E-plane
- 270 degree
Amplitude [mV]
Time [ns]
Belt E-plane
- 90 degree
Amplitude [mV]
Time [ns]
Belt E-plane
- 180 degree
Amplitude [mV]
Time [ns]
(b)

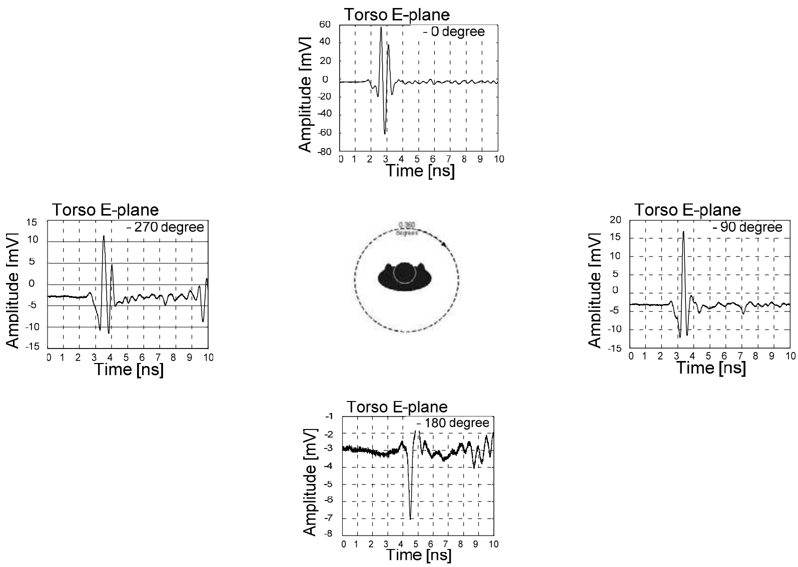

(c)

Figure 6. Example of measured time signals at 0, 90, 180 and 270 degrees for three scenarios (E-plane), (a) head, (b) torso, and (c) belt.

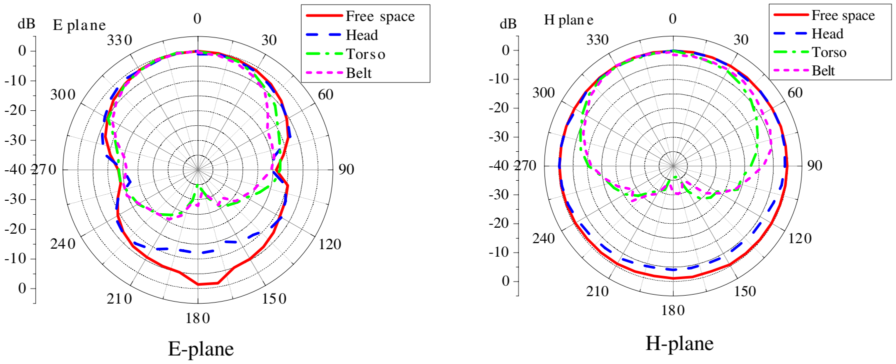

Figure 7. Normalized peak to peak voltage in dB vs. azimuth in degrees.

for torso and belt scenarios.

With the antenna close to the belt and torso, we observe a strong attenuation of the back radiation in both planes, whereas the blockage effect caused by having the antenna near the head seems to be less important.

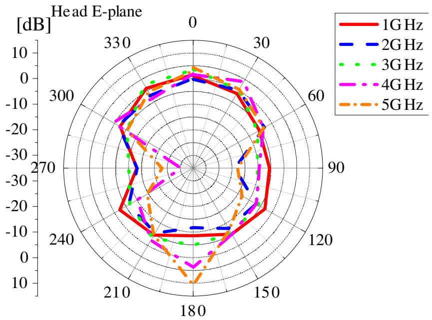

Figure 8. Radiation patterns at selected frequencies, head scenario, E plane.

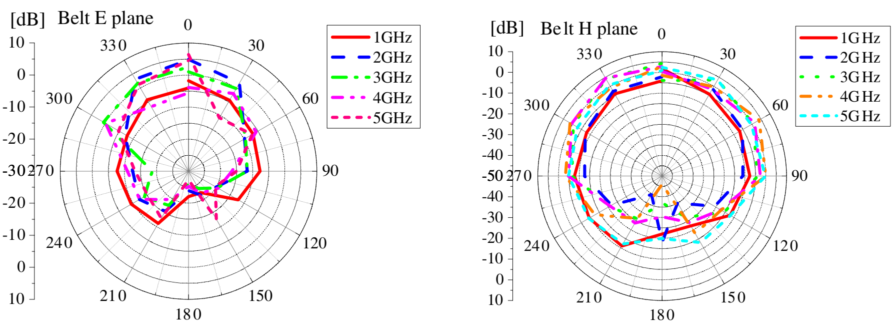

Figure 9. Radiation patterns at selected frequencies, belt scenario, E and H planes.

The measurement results can also be interpreted by investigating the frequency domain properties of the received signals. Table 1 and Figs. 8 to 10 illustrate the frequency dependency of the body effect on the antenna radiation patterns.

No apparent blockage effect can be seen in the case where the antenna is placed near the head (Fig. 8). The patterns are what one would expect of a dipole apart from the back radiation (180 degrees) where the magnitude seems to increase with frequency.

For the belt and torso scenarios, the blockage caused by the body increases with frequency in both E and H planes.

For the antenna on a torso and on a belt scenario, pulse waveforms become different for angle approximately from 140° till 220°. These angles are corresponding to backward antenna radiation. A peak-to-peak amplitude for an antenna on a torso or on a belt for angle 180° is about 2–4 mV, which can be assumed as noise in comparison with

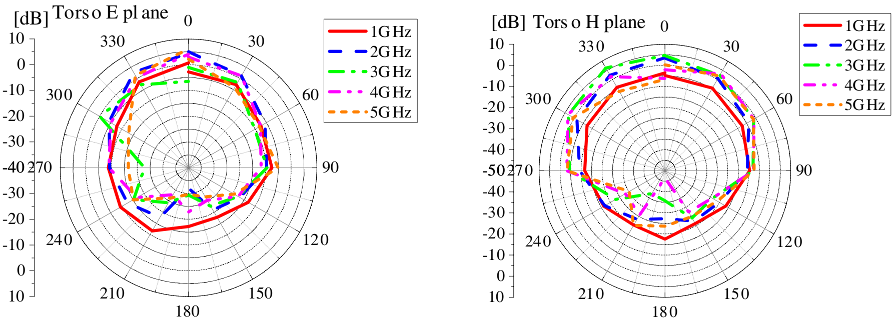

Figure 10. Radiation patterns at selected frequencies, torso scenario, *E* and *H* planes.

Table 1. Frequency dependency of the body effect on the antenna radiation patterns.

***E*-plane**	**Head** attenuation [dB]				**Torso** attenuation [dB]				**Belt** attenuation [dB]			
	0°	**90°**	**180°**	**270°**	**0°**	**90°**	**180°**	**270°**	**0°**	**90°**	**180°**	**270°**
1 GHz	1	−5.5	−8.5	−13	−2.7	−7.5	−17	−8.7	−1.8	7.7	−22	−7.7
2 GHz	−0.3	−18	−11	−13	5	−9.5	−32	−9.2	5	11	−23	−12
3 GHz	3.6	−10	−5	−10	−1.1	−9.5	−30	−22	1	11	−26	−18
4 GHz	1.5	−9.5	3.7	−30	−3	−11	−22	−9	−4	16	−25	−11
5 GHz	4.3	−18	10	−23	2	−5	−30	−16	6.3	15	−27	−13

a forward radiation where peak to peak amplitude is about 100 mV–140 mV.

At 4 GHz, we can see strong backward blockage, about −40 dB for a torso and belt scenarios. At low frequency (1 GHz) is the smaller blockage −20 dB level.

5. CONCLUSION

In this paper, we have investigated and quantified the effect of the human body on the radiation pattern of an UWB antenna. Three antenna locations on the body where considered; the head, the torso and the belt. In all cases, both *E* and *H* planes radiation patterns were measured.

These measurements show that the main effect of the body on the antenna radiation is blockage. The minimal blockage occurs when the antenna is located near the head. It is around 5 dB–10 dB loss for all polarisations. The torso and belt scenarios have much loss spatially for a backward and sideward radiations. The losses are from about 10 dB to 35 dB, for both polarisations.

The signal blockage is dependent on the antenna polarization. For vertical and horizontal polarizations, signal blockages are different for backward and side radiations. Horizontally polarized antenna (all scenarios are included) has the aria approximately from 300° till 60° (from 2 GHz to 5 GHz) on a forward radiation, where a signal value is around −20 dB (Figs. 8–10). In a case of an antenna on a head scenario, we have backwards radiation as well for the aria of about 120° to 240°.

The described blockage effect should be taken into account by UWB PAN system design.

REFERENCES

1. Win, M. Z. and R. A. Scholtz, "Impulse radio: How it works," *IEEE Communications Letters*, Vol. 2, No. 2, 36–38, February 1998.
2. Klemm, M. and G. Tröster, "EM energy absorption in the human body tissues due to UWB antennas," *Progress In Electromagnetics Research*, Vol. 62, 261–280, 2006.
3. Alvarez, A., G. Valera, M. Loberia, and R. Torres, "New channel impulse response model for UWB indoor system simulations," *IEEE VTC*, 1–5, April 2003.
4. Nielsen, J. O. and G. F. Pedersen, "In network evaluation of body carried mobile terminal performance," *Proc. 12th PIMRC*, Vol. 1, D.109–D.113, September 2001.
5. Nielsen, J. O., G. F. Pedersen, K. Olesen, and I. Z. Kovacs, "Statistic of measured body loss for mobile phones," *IEEE Transaction on Antennas and Propagation*, Vol. 49, 1351–1353, September 2001.
6. Kotterman, W. A. T., G. F. Pedersen, K. Olesen, and P. Eggers, "Cable-less measurement set up for wireless handheld terminals," *Proc. 12th International Symposium on Personal in Door and Mobile Radio Communication (PIMRC)*, Vol. 1, B.112–B.116, September 2001.
7. Alomainy, A., Y. Hao, C. G. Parini, and P. S. Hall, "Comparison between two different antennas for UWB on-body propagation measurements," *Antennas and Wireless Propagation Letters*, Vol. 4, 31–34, 2005.
8. Welch, T. B., R. L. Musselman, B. A. Emessiene, P. D. Gift, D. K. Choudhury, D. N. Cassadine, and S. M. Yano "The

effects of the human body on UWB signal propagation in an indoor environment," *IEEE Journal on Selected Areas in Communications*, Vol. 20, No. 9, 1778–1782, December 2002.

9. De Jongh, R. V., A. G. Yarovoy, L. P. Ligthart, I. V. Kaploun, and A. D. Schukin, "Design and analysis of new GPR antenna concepts," *Proceedings, Seventh International Conference on Ground-Penetrating Radar*, Vol. 1, 81–86, Lawrence, USA, 1998.
10. Yarovoy, A. G., R. Pugliese, J. R. Zijderveld, and L. P. Ligthart, "Antenna development for UWB impulse radio," *34th European Microwave Conference*, 1257–1260, Amsterdam, Netherlands, 2004.
11. Gemio, J., J. Parron, and J. Soler, "Human body effects on implantable antennas for ism bands applications: Models comparison and propagation losses study," *Progress In Electromagnetics Research*, Vol. 110, 437–452, 2010.
12. Vergés, J., J. Anguera, C. Puente, and D. Aguilar, "Analysis of the human body on the radiation of FM handset antenna," *Microwave and Optical Technology Letters*, Vol. 51, No. 11, 2588–2590, November 2009.
13. Pladevall, A., C. Picher, A. Andújar, and J. Anguera, "Some thoughts on human body effects on handset antenna at the FM band," *Progress In Electromagnetics Research M*, Vol. 19, 121–132, 2011.